

Observation of Positronium Specular Reflection from LiF

M. H. Weber,⁽¹⁾ S. Tang,⁽¹⁾ S. Berko,⁽²⁾ B. L. Brown,^{(3),(a)} K. F. Canter,⁽²⁾ K. G. Lynn,⁽⁴⁾
A. P. Mills, Jr.,⁽³⁾ L. O. Roellig,⁽¹⁾ and A. J. Viescas^{(1),(b)}

⁽¹⁾City University of New York, New York, New York 10036

⁽²⁾Brandeis University, Waltham, Massachusetts 02154

⁽³⁾AT&T Bell Laboratories, Murray Hill, New Jersey 07974

⁽⁴⁾Brookhaven National Laboratory, Upton, New York 11973

(Received 26 July 1988)

A monoenergetic positronium (Ps) beam of 0–60-eV energy and an angular width of $\pm 5^\circ$ is created by charge-exchange collisions of a slow positron beam passing through an Ar gas cell. The Ps beam is directed at a LiF(100) crystal, and reflected Ps atoms are detected at an annihilation target. With angles of incidence of 50° to 60° we observe a specularly reflected beam with a maximum reflected fraction $R = (30 \pm 5)\%$ at a Ps energy of 7 eV. At higher energies (20–60 eV) the reflectivity ($R = 0.5\%$ at 60 eV) can be ascribed principally to a short Ps mean free path $\lambda = (0.75 \pm 0.15) \text{ \AA}$, and to a lesser extent a Ps inner potential of about 4 eV.

PACS numbers: 36.10.Dr, 61.14.Hg, 71.60.+z, 79.20.Rf

Scattering experiments employing various subatomic and atomic particles have proven to be valuable in the study of surfaces. The most widely used technique is low-energy electron diffraction (LEED), particularly since computations are now successful in accounting for the multiple scattering of electrons from the inner atomic layers.¹ Neutral molecules and atoms like H_2 and He interact mainly with surface atoms, but the few meV beams typically used in diffraction experiments are not energetic enough to probe small-scale surface structure that does not affect the long-range part of the van der Waals surface potential.² On the other hand, the large He mass is especially suited to the study of inelastic effects.³ Positronium (Ps), the bound state of a positron and an electron, should interact more intimately with a surface than He because of its much larger energy for a given wavelength. Furthermore, at energies above its 6.8-eV binding energy Ps is expected to break up with high probability upon scattering from a solid, and unlike electron scattering, Ps collisions should be confined to the outermost surface layers. Thus low-energy Ps diffraction (LEPD) could be a unique probe of ordered surfaces,⁴ combining some of the best characteristics of both LEED and He diffraction. The most important experimental question is whether the elastic scattering of energetic Ps is sufficiently intense to make LEPD possible with Ps beams presently available.⁵ In this Letter we describe the first measurement of the angle-resolved Ps reflection from a solid surface. We find that for LiF(100) there is a significant reflection probability for energies up to 60 eV and that LEPD studies should indeed be feasible.

Our Ps beam is produced by positrons undergoing charge-exchange collisions with Ar atoms.⁶ If we consider only events in which the Ar ion and the Ps atom are formed in their ground states, the Ps will be essentially

monoenergetic because of the negligible recoil energy of the heavy ion. Since an energy of 15.7 eV is required to remove an electron from Ar, the threshold energy for positrons to form Ps is $E_{\text{th}} = 15.7 - 6.8 = 8.9$ eV. Ps formed in excited states will also be present. Using the calculated⁷ formation probability of 2S Ps and the expected large total collisional cross section of Ps excited states, we estimate that the excited-state contamination of our beam is about 5%. The contamination of the energy purity of the Ps beam due to Ar excitation⁸ is estimated to be less than 1%.

Our slow positron beam⁹ has an initial longitudinal energy spread of 0.4 eV (10% to 90%) when accelerated to 150 eV. The Ps beam is formed by sending the positrons through a differentially pumped gas cell filled with Ar gas of 99.995% nominal purity at a pressure of 10^{-3} Torr. The background pressure in the experimental chamber is about one percent of the gas-cell pressure. A schematic drawing of the experimental apparatus is shown in Fig. 1. The grid at potential V_1 is used to gate the positron beam during the background measurements. The gas cell, gc, is electrically floated to a potential V_2 to change the kinetic energy, E_+ , of the 150-eV positrons entering the gas cell, and thus the Ps beam energy, $E_{\text{Ps}} = E_+ - E_{\text{th}}$. A positive potential, V_3 , applied to a tube following the gas cell rejects the positrons from the sample chamber, but does not stop the Ps atoms. The sample, s, and the detector, d, can be rotated independently about a common axis perpendicular to the plane of the drawing. The sample is held at a temperature of a few hundred degrees Celsius to prevent impurities from accumulating on the surface. Ps atoms are detected when they strike an annihilation plate, a, an inoperative channel electron multiplier array. The annihilation photons are observed in coincidence by a pair of bismuth germanate (BGO) scintillators, placed outside of the

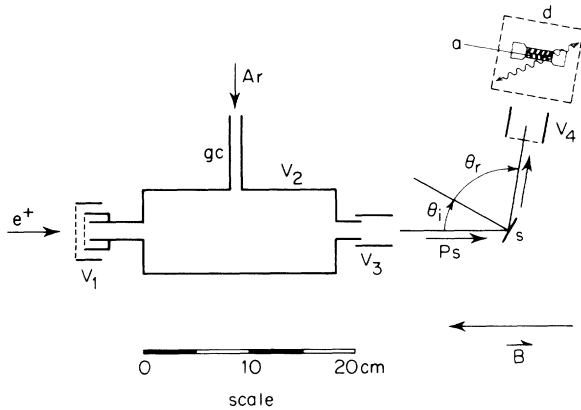


FIG. 1. The experimental setup as seen from above. Ps is formed in a stainless-steel gas cell (gc) filled with Ar at a pressure of 10^{-3} Torr. Electrically floated tubes and grids can have positive potentials to repel positively charged particles. The sample (s) and the detector (d) can be rotated independently around the same axis. The detector consists of an annihilation plate (a) inside the vacuum chamber and two external BGO scintillators above and below, outlined by a dashed line.

vacuum chamber above and below the annihilation plate. Lead and tungsten shields reduce the background due to annihilations coming from the gas cell and from the sample. The grid at a potential $V_4 = +200$ V prevents positrons from striking the annihilation plate. The annihilation plate and BGO detectors can be rotated through an angle from 100° to 180° from the axis of the Ps beam. In the 180° position and with the sample removed, the annihilation plate and BGO detectors monitor the incident Ps beam. The Ps atoms traverse the same distance prior to detection in this configuration as in the reflection measurement. We therefore divide our Ps reflection intensity by the straight-through Ps beam intensity taken at the same Ps energy to find the absolute Ps reflection coefficient. We also correct for the fraction of the Ps beam missing the sample for angles of incidence greater than 50° . The straight-through (180°) Ps beam intensity increases with energy until it reaches a broad maximum at 60 eV.

The angular distribution of the scattered Ps was measured by keeping the total scattering angle $\psi = \theta_i + \theta_r$, the sum of the incident and reflected angles, constant during a measurement and changing θ_i (and thereby θ_r) by rotating the sample. Data were taken at angles $\psi = 100^\circ$, 120° , and 130° . The estimated error in the setting of ψ is $\pm 4^\circ$. The Ps energy was held constant while θ_i was varied around the specular condition $\theta_i = \theta_r = \psi/2$. The results are shown in Fig. 2. The data have been normalized and a background obtained for negative θ_i has been subtracted. The narrow peak near the specular angle and the absence of scattering away from the specular condition is our primary evidence for

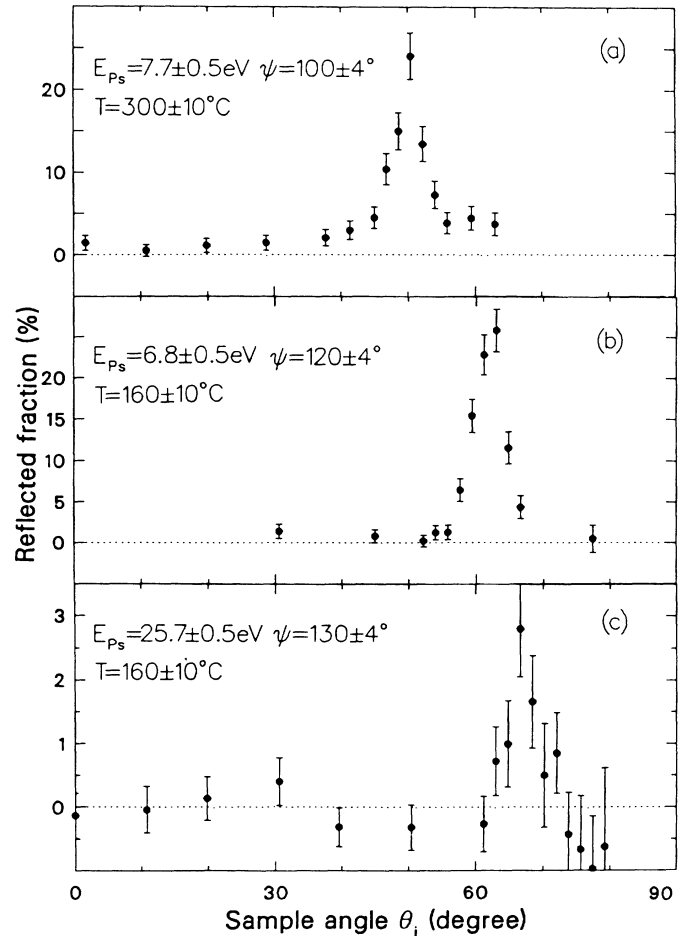


FIG. 2. Reflection probability of Ps at constant incident energy and total scattering angle $\psi = \theta_i + \theta_r$ vs the incident angle θ_i .

elastic Ps reflection from the LiF crystal. The fact that we do not encounter a large isotropic background means that the probability of Ps scattering inelastically into the detector solid angle is insignificant. The observed 5° full width at half maximum of the peaks is in agreement with an estimate of the width due to geometrical effects alone. A second data set shown in Fig. 3 is the reflection probability versus Ps energy taken while holding the angles constant near the specular condition. The maximum Ps reflection coefficient R is 30% and 21% at $\psi = 100^\circ$ and 120° , respectively. At energies higher than 7 eV the reflected fraction decreases to about 0.5% at 60 eV, the highest energy examined.

Tests were made to determine whether the observed specular reflection depended on the surface condition of the sample. The sample was exposed to air and put back into the vacuum without heating either the chamber or the sample. At room temperature there was some evidence for reflection, but the intensity was so low that we could not establish whether it was specular or not. Upon

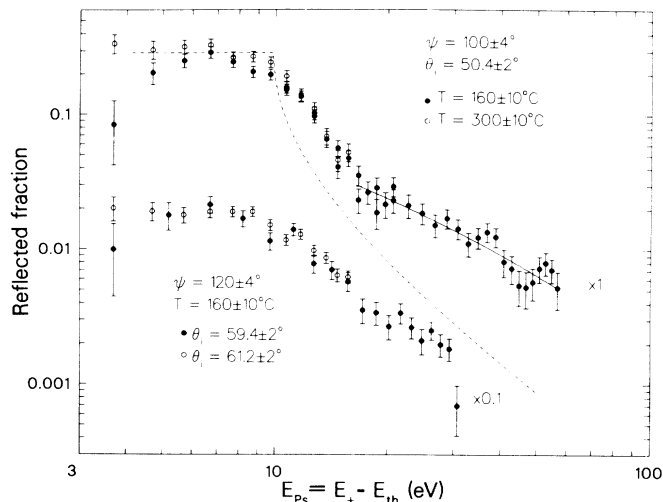


FIG. 3. Ps reflection probability vs the incident Ps energy. The solid line is calculated with use of Eq. (3) with $V_0=4$ eV and λ taken from the fitted line in Fig. 4. The dashed line is calculated with $V_0=4$ eV and $\lambda=\infty$.

our increasing the sample temperature, the reflected intensity increased monotonically to a value of 30% at 300°C for $\psi=100^\circ$. We interpret this to mean that surface contaminants that destroyed the specular reflection by contributing to diffuse scattering were removed by heating the LiF. Indeed, the long lifetime of Ps in powdered insulators¹⁰ implies that the reflection probability at low energies (a few eV) should be near unity. It may well be that the Ps reflectivity of a LiF sample cleaved under ultrahigh-vacuum conditions would show a much higher reflectivity as was observed in a positron reflectivity measurement.¹¹ In another test, we observed no specular reflection from an untreated polycrystalline Cu sample at 160°C. Finally, positrons implanted directly into the LiF sample caused the emission of a broad distribution of Ps unlike the narrow specular peaks shown in Fig. 2.

A theoretical interpretation of the Ps reflection probability and its energy dependence shown in Fig. 3 would be helpful as a basis for future work. Unfortunately, we know of no calculations that would be applicable to Ps reflection from LiF. We therefore consider the simplest possible model, Ps reflection from a potential step of height V . The real part of V is the inner potential which we estimate to be $V_0=4$ eV taking into account the 3-eV binding energy of Ps inside the LiF.¹² The reflection probability is

$$R = R_0 \left| \frac{k_i - k_0}{k_i + k_0} \right|^2, \quad (1)$$

where k_i and k_0 are the perpendicular components of the Ps wave vectors inside and outside the crystal, and where we include a factor R_0 to account for the reflection prob-

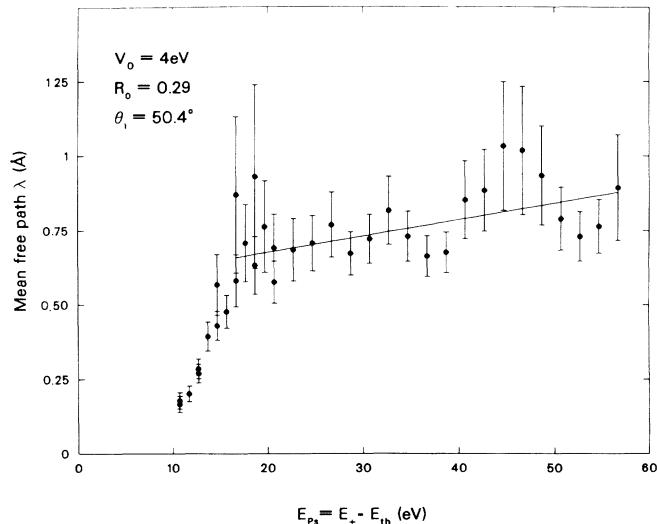


FIG. 4. Ps mean free path estimated from Fig. 3. The straight line is a least-squares fit of $\lambda = \lambda_0 + aE_{Ps}$ to the data in the interval $16.5 \text{ eV} < E_{Ps} < 56.7 \text{ eV}$. The fitted parameters are $\lambda_0 = (0.57 \pm 0.06) \text{ \AA}$ and $a = (0.0044 \pm 0.0017) \text{ \AA eV}^{-1}$, with a χ^2 per degree of freedom $\chi^2/\nu = 15.26/26$.

ability being less than unity at low energies. If we include only the real part of V , we do not predict the observed energy dependence of the reflection probability: R equals R_0 for Ps energies less than $V_0/\cos^2\theta_i$, but it falls off sharply for higher energies, and finally approaches a $1/E_{Ps}^2$ dependence. There is evidently much more scattering than can be accounted for by the real part of the inner potential alone. We can obtain a better fit to the data by adding an energy-dependent imaginary part, V_i , to the potential. The wave vector inside the crystal acquires an imaginary part κ which is related to V_i by the equation

$$V_i = -[\hbar^2\kappa^2 + (E - V_0)2m_{Ps}]^{1/2} \hbar\kappa/m_{Ps}, \quad (2)$$

where $m_{Ps} \approx 2m_e$ is the Ps effective mass, and $E = E_{Ps} \times \cos^2\theta_i$. We can solve Eq. (1) for the value of κ that gives as a certain reflectivity R at a given energy E :

$$\kappa^2 = \frac{m_{Ps}}{\hbar^2} [E(\rho^2 - 2) + V_0 + \rho(E^2\rho^2 - 2EV_0)^{1/2}], \quad (3)$$

where $\rho = (R_0 + R)/(R_0 - R)$. Using the data of Fig. 3 and a constant $V_0=4$ eV as given quantities, we calculate κ and the corresponding mean free path, $\lambda = (2\kappa \times \cos\theta_i)^{-1}$. The result plotted in Fig. 4 is consistent with a nearly constant $\lambda \approx 0.75 \text{ \AA}$ for $E_{Ps} > 20$ eV, in agreement with our expectation that the Ps is readily ionized during its collision with the surface. The solid line in Fig. 4 is a two parameter fit to the data that suggests λ is slowly increasing with energy. The solid line in Fig. 3 is the corresponding reflectivity calculated with

use of Eq. (3); the dashed line was calculated with $\lambda = \infty$ and $V_0 = 4$ eV. The absence of sharp Bragg peaks in Fig. 3 also seems to indicate that the Ps is only interacting with the outer layer of the surface. A very broad Bragg contribution at low E_{Ps} cannot be ruled out, however. Such a component could be responsible for the change in slope in the reflectivity versus E_{Ps} (Fig. 3) at about 15 eV, and would cause the unphysically small λ below 15 eV in our analysis. The reasonably high-elastic Ps reflection probability observed even at high energies, in spite of the presence of the large absorptive potential, is in retrospect not surprising in view of the requirements of unitarity.¹³

In conclusion, we have observed the specular reflection of Ps, and established that there is enough intensity at high energies to make further study worthwhile. Although the scattering appears to be restricted to the outermost surface, one should be able to see diffracted beams at higher orders as a result of the periodicity of the surface. A program is presently underway to improve the Ps beam intensity and the detector geometry in order to observe nonspecular diffraction. The effect of adsorbates on the attenuation of the specular beam should be systematically studied.¹⁴ It will be interesting to see if metals also have a large reflection coefficient for Ps, since, unlike LiF, a metal has no Ps bound state in the bulk.

The authors would like to thank Dr. M. J. Cardillo and Dr. P. M. Platzman for interesting discussions and J. J. Hurst for technical assistance. This work was supported in part by the National Science Foundation (Grant No. DMR-8620168), and in part by the Division of Materials Sciences, U.S. Department of Energy, under Contract No. DE-AC-76CH0016.

^(a)Present address: Department of Physics, Harvard University, Cambridge, MA 02138.

^(b)Present address: Department of Physics, Brookhaven National Laboratory, Upton, NY 11973.

¹See, for example, F. Jona, *J. Phys. C* **11**, 4271 (1978); C. B. Duke, in *Surface Properties of Electronic Materials*, edited by D. A. King and D. P. Woodruff (Elsevier, New York, 1986), Chap. 3; and A. Kahn, *Surf. Sci. Rep.* **4/5**, 193 (1983).

²H. Hoinkes, *Rev. Mod. Phys.* **52**, 933 (1980).

³G. Brusdeylins, R. B. Doak, and J. P. Toennies, *Phys. Rev. Lett.* **46**, 1138 (1980).

⁴K. F. Canter, in *Positron Scattering in Gases*, edited by J. W. Humberston and M. R. C. McDowell (Plenum, New York, 1984), p. 219.

⁵L. O. Roellig *et al.*, in *Atomic Physics with Positrons*, edited by J. W. Humberston and E. A. G. Armour (Plenum, New York, 1987), p. 233; G. Laricchia *et al.*, *ibid.*, p. 223.

⁶B. L. Brown, in Ref. 5, p. 241, and in *Positron Annihilation*, edited by P. C. Jain, R. M. Singru, and K. P. Gopinathan (World Scientific, Singapore, 1985), p. 328.

⁷P. Khan, P. S. Mazumdar, and A. S. Ghosh, *J. Phys B* **17**, 4785 (1985).

⁸W. E. Kauppila and T. S. Stein, in Ref. 5, p. 27.

⁹K. G. Lynn *et al.*, in Ref. 5, p. 161.

¹⁰R. Paulin and G. Ambrosino, *J. Phys. (Paris)* **29**, 263 (1968).

¹¹A. P. Mills, Jr., and W. S. Crane, *Phys. Rev. B* **31**, 3988 (1985).

¹²A. Dupasquier, in *Positron Solid State Physics*, edited by W. Brandt and A. Dupasquier (North-Holland, Amsterdam, 1983), p. 510.

¹³Unitarity requires inelastic scattering to be accompanied by elastic scattering: see, for example, P. Roman, *Advanced Quantum Theory* (Addison-Wesley, Reading, MA, 1965), p. 198.

¹⁴B. Poelsema, S. T. deZwart, and G. Cosma, *Phys. Rev. Lett.* **49**, 578 (1982).